Int. J. Simul. Multidisci. Des. Optim. **2**, 77–82 (2008)

DOI: 10.1051/smdo:2008010

Available online at:
http://www.ijsmdo.org

Analysis of a hybrid composite tank under pressure

A. Hocine[1,2,a], D. Chapelle[2], A. Benamar[3] and A. Bezazi[4]

[1] University Hassiba Benbouali of Chlef BP. 151, Chlef 02000, Algeria
[2] Institut FEMTO-ST, Dept. LMARC, 24, rue de l'épitaphe, 25000 Besançon, France
[3] ENSET, Department of mechanical engineering, BP 1523, Oran 31000, Algeria
[4] University 08 Mai 1945, BP. 401, Guelma 24 000, Algeria

Received 25 July 2007, accepted 11 February 2008

Abstract – In this work, the analysis of a hybrid composite tank of storage of hydrogen is presented. This solution made of a carbon/epoxy envelope coated on a metal liner and an intermetallic material is proposed. Each layer of the laminate is assumed to be anisotropic, and liner and intermetallic were assumed to be isotropic. This work is concerned with the study of the elastic behaviour of this solution. Based on the three-dimensional (3-D) elasticity, an exact solution for the stresses, strain and displacement is presented. The effect of stacking sequences on the behaviour of hybride solution is presented.

1 Introduction

Hydrogen is considered as one of the more promising energy vectors of the future. It can be used as a fuel in many applications. However, this requires that several technological hurdles are cleared especially the one concerning its storage. Storage must offer a high degree of safety as well as allowing ease of use in terms of energy density and dynamics of fuel storage and controlled release [1].

As everyday use of such storage, we mention the cases of oxygen in hospitals and various gases in the university laboratories or industrial ones. The pressure of the compressed hydrogen is generally about 350 bars (35 MPa), which leads to reach a convincing mass density for the composite tanks. However, the density of storage remains low, and in order to make this technology competitive it is necessary to reach a pressure of 700 bars. At present, the thin-walled or thick tanks are largely used in several branches of engineering [3], such as the storage of compressed hydrogen, compressed and liquefied natural gas [4].

The hyperbare storage of hydrogen must take into account some important characteristics such as explosiveness, inflammability and the low value of hydrogen atom's radius. To improve the performances of this type of storage, research is mainly concerned with two aspects: powerful materials for both the structure and the internal coating of the tanks as well as economical manufacturing techniques [2].

Several storage models of hydrogen were proposed. Xia et al. [5] provide an analytical model for research and analysis of the mechanical properties of a multi-layer tube under mechanical loading. Chapelle and Perreux [6] present a paper which purpose is to study the cylindrical section of a Type 3 high-pressure hydrogen storage vessel, combining an aluminium liner which prevents gas diffusion and an overwrapped composite devoted to reinforce the structure. The laminate composite is assumed to be an elastic damageable material whereas the liner behaves as an elastic plastic material. Based on the classical laminate theory and on Hill's criterion to take into account the anisotropic plastic flow of the liner, the model provides an exact solution for stresses and strains on the cylindrical section of the vessel under thermomechanical static loading. Takeichia et al. [7] propose a novel hydrogen storage vessel with the lightness and smallness, a "hybrid hydrogen storage vessel", which is a combination of a lightweight high-pressure vessel and hydrogen storage alloy. This model is expected to solve the problem of hydrogen storage techniques in weight and volume other than the techniques using compressed hydrogen or hydrogen storage alloy, individually.

In this work, a hybrid prototype of storage is proposed. It consists of an carbon/epoxy envelope coated on a metal liner and hydride intermetallic material. The intermetallic aims to absorb hydrogen coming from microcracks, as those formed by hydrogen embrittlement of the aluminium liner. Interest of the site of the intermetallic directly placed at the contact of the aluminium liner, since the reinforced carbon fiber layer, the alloy expansion will mainly occurs towards the inside (e.g. the aluminium liner).

This work focus on the study of the elastic behaviour of a hybrid composite storage solution. The effect of the stacking sequence, on the structure stiffness may then be investigated. An analysis of the stresses, strains and the displacements through the wall's thickness is presented.

[a] Corresponding author: hocinea_dz@yahoo.fr

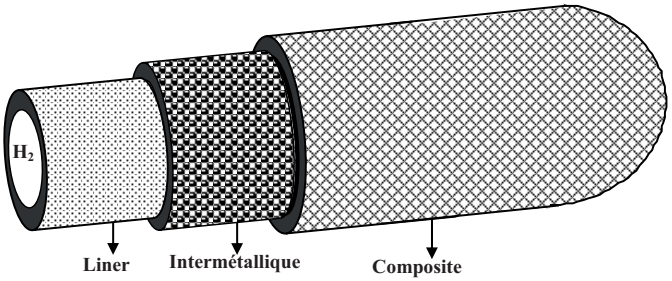

Fig. 1. Hybrid solution.

2 Analysis procedure

2.1 Stress and strain analysis

The stress and strain analysis of a cylindrical tube with internal and external radius r_0, r_a respectively subjected to an axisymmetric internal pressure is performed. The metal liner is reinforced with a composite material manufactured by the filament winding process, and an intermediate layer of intermetallic is added between the previous layers, as indicated in Figure 1.

The stress/strain relation of the kth layer of an anisotropic material can be written [8]:

$$\begin{Bmatrix} \sigma_z \\ \sigma_\theta \\ \sigma_r \\ \tau_{\theta r} \\ \tau_{z r} \\ \tau_{z \theta} \end{Bmatrix}^{(k)} = \begin{bmatrix} C_{11} & C_{12} & C_{13} & 0 & 0 & C_{16} \\ C_{12} & C_{22} & C_{23} & 0 & 0 & C_{26} \\ C_{13} & C_{23} & C_{33} & 0 & 0 & C_{36} \\ 0 & 0 & 0 & C_{44} & C_{45} & 0 \\ 0 & 0 & 0 & C_{45} & C_{55} & 0 \\ C_{16} & C_{26} & C_{36} & 0 & 0 & C_{66} \end{bmatrix}^{(k)} \begin{Bmatrix} \varepsilon_z \\ \varepsilon_\theta \\ \varepsilon_r \\ \gamma_{\theta r} \\ \gamma_{z r} \\ \gamma_{z \theta} \end{Bmatrix}^{(k)} \tag{1}$$

where σ_z, σ_θ, and σ_r are axial, circumferential, and radial stresses respectively; $\tau_{z\theta}$, τ_{zr}, and $\tau_{\theta r}$ are shear stresses in the planes z–θ, $z-r$, θ–r respectively; k is the number of the considered layer; $\boldsymbol{C}_{11}$-$\boldsymbol{C}_{66}$ are rigidity coefficients of the kth layer, ε_z, ε_θ, and ε_r are axial, circumferential, and radial strains respectively; $\gamma_{\theta r}$, γ_{zr}, and $\gamma_{z\theta}$ are the shear strains in the planes θ–r, $z-r$, and z–θ respectively.

The asymmetric loading of the hybrid tube allows reducing the equilibrium equations in the cylindrical coordinates; they are expressed as [5]:

$$\begin{cases} \frac{d\sigma_r^{(k)}}{dr} + \frac{\sigma_r^{(k)} - \sigma_\theta^{(k)}}{r} = 0 \\ \frac{d\tau_{\theta r}^{(k)}}{dr} + \frac{2}{r}\tau_{\theta r}^{(k)} = 0 \\ \frac{d\tau_{zr}^{(k)}}{dr} + \frac{\tau_{zr}^{(k)}}{r} = 0. \end{cases} \tag{2}$$

Strain/displacement relations are expressed as [5]:

$$\begin{cases} \varepsilon_r^{(k)} = \frac{dU_r^{(k)}}{dr}\ ,\ \varepsilon_\theta^{(k)} = \frac{U_r^{(k)}}{r}\ ,\ \varepsilon_z^{(k)} = \frac{dU_z^{(k)}}{dz} = \varepsilon_0 \\ \gamma_{zr}^{(k)} = 0\,,\ \gamma_{\theta r}^{(k)} = \frac{dU_\theta^{(k)}}{dr} - \frac{U_\theta^{(k)}}{r}\ ,\ \gamma_{z\theta}^{(k)} = \frac{dU_\theta^{(k)}}{dz} = \gamma_0 r. \end{cases} \tag{3}$$

Substituting equation (1) into equation (2) and using equation (3), the following differential equation is obtained:

$$\frac{d^2U_r^{(k)}}{dr^2} + \frac{1}{r}\frac{dU_r^{(k)}}{dr} - \frac{N_1^{(k)}}{r^2}U_r^{(k)} = \alpha_1^{(k)}\frac{\varepsilon_0}{r} + \alpha_2^{(k)}\gamma_0 \tag{4}$$

with

$$\beta^{(k)} = \sqrt{N_1^{(k)}} = \sqrt{C_{22}^{(k)}\Big/C_{33}^{(k)}}. \tag{5}$$

The solution of equation (4) takes the form:
If $\beta^{(k)} = 1$ then

$$U_r^{(k)} = D^{(k)}r + E^{(k)}/r \tag{6}$$

If $\beta^{(k)} \neq 1$ then

$$U_r^{(k)} = D^{(k)}r^{\beta^{(k)}} + E^{(k)}r^{-\beta^{(k)}} + \alpha_1^{(k)}\varepsilon_0 r + \alpha_2^{(k)}\gamma_0 r^2 \tag{7}$$

with

$$\begin{aligned} \alpha_1^{(k)} &= \frac{C_{12}^{(k)} - C_{13}^{(k)}}{C_{33}^{(k)} - C_{22}^{(k)}} \\ \alpha_2^{(k)} &= \frac{C_{26}^{(k)} - 2\,C_{36}^{(k)}}{4\,C_{33}^{(k)} - C_{22}^{(k)}}. \end{aligned} \tag{8}$$

2.2 Boundary conditions

The boundary conditions are imposed by the geometry conditions of the structure, due to continuity and volume conservation, and by the conditions of loading. It is assumed that there are no slips in the interfaces and that there is continuity of stresses and displacements. These boundary conditions allow to determine the integration constants $D^{(k)}$, $J^{(k)}$, γ_0 and ε_0.

The number of unknown factors, or integration constant of the system, to be solved is 2 $(z+1)$ for z layers of the hybrid solution; where D^k, E^k, γ_0 and ε_0 for $k \in [1,\ z]$.

The radius $r_{int}(k)$ and $r_{ext}(k)$ are introduced for each layer $k$and it is noted that

$$r_{int}^{(k=)} = r_0 \ \ et \ \ r_{ext}^{(k=z)} = r_a. \tag{9}$$

➢ The condition of continuity of radial displacements results in the relation is:

$$\forall\, k \in [1,\ z-1]\,, \quad U^{(k)}(r_{ext}(k)) = U^{(k+1)}(r_{ext}(k)). \tag{10}$$

➢ The condition of continuity of radial stress results in the relation is:

$$\begin{aligned} &\forall\ k \in [1,\ z-1]\,, \quad \sigma_r^{(k)}(r_{ext}(k)) = \sigma_r^{(k+1)}(r_{ext}(k)), \\ &\sigma_r^{(k=)}(r = r_0) = -p_0, \\ &\sigma_r^{(k=z)}(r_{ext}(z)) = 0. \end{aligned} \tag{11}$$

Table 1. Elastic parameters.

Properties	Carbon/Epo xy (T300 /934)	Liner Aluminium	Intermetallic (Zr_3Fe)
E_x (GPa)	141,6	69,5	122.5
E_y (GPa)	10,7	69,5	122.5
G_{xy} (GPa)	3,88	26,7	45.79
ν_{yx}	0,268	0,3	0.3375
ν_{zy}	0,495	–	–

➢ The equilibrium condition of axial force due internal pres-sure with end loading effect

$$2\,\pi \sum_{k=1}^{z} \int_{r_{k-1}}^{r_k} \sigma_z^{(k)}(r)\, r\, dr = \pi\, r_0^2\, p_0 + F \tag{12}$$

where F is the applied axial load.
➢ Torque balance is

$$2\,\pi \sum_{k=1}^{z} \int_{r_{k-1}}^{r_k} \tau_{z\theta}(r)\, r^2 dr = C \tag{13}$$

where C is the applied torque.

The hypothesis of this study neglects torque and axial loads, where $F = 0$ and $C = 0$. Thus one has 2 (z) equations to identify the whole integration constants. In the continuation, one endeavours to write the components of matrix A and of the vector B of the linear problem are equivalent such as:

$$A \times X = B \tag{14}$$

with: $X = \begin{pmatrix} D^1 \\ D^2 \\ . \\ . \\ D^z \\ E^1 \\ E^2 \\ . \\ . \\ E^z \\ \varepsilon_0 \\ \gamma_0 \end{pmatrix}$.

2.3 Geometry and resolution

The tube is characterised by an internal radius of 50 mm, a liner thickness of 0.5 mm, 0.1 mm for the intermetallic and 0.5 mm of each layer of the laminate. The properties of materials are presented in the table 1 below.

Table 2 presents the stacking sequence of the different studied laminates, where the order of the stacking of each laminate is taken from interior to exterior.

The internal wall of the hybrid tube is subjected to internal pressure of 10 MPa. All results are presented through wall's thickness of the solution.

Table 2. Different stacking sequences of the composite tube.

Composites Sequence types	Angle of wrap
Seq1	[+55/−55/+55/−55]
Seq2	[+55/−30/+30/−55]
Seq3	[+55/−55/+30/−30]

3 Results and discussions

3.1 Stress analysis

Figures 2–4 show the distribution of the axial, circumferential, radial and shear stresses σ_z, σ_θ, σ_r and $\tau_{z\theta}$ respectively through the wall's thickness for the three sequences. It can be also noticed that the change of the properties from one layer to another influences the overall mechanical behaviour.

3.1.1 Hoop and axial stress

As shown in Figure 2, it is obvious that the hoop and axial stresses of cylindrical tank have discontinuous variations at the interfaces with different materials. Figure 2 shows that the presence of intermetallic in this work induced maximal hoop and axial stress for $(52 \leqslant r \leqslant 52.1)$ for the three sequences. The analysis shows for all sequence that the curves of the Hoop and axial Stress for the laminate Seq1 are below than the Seq2 and Seq3.

3.1.2 Shear stress

Figure 3 shows the shear stress $\tau_{z\theta}$ through the radius for the three sequences and has the same trend, but differs in values and occurs in five stages starting from the internal wall to the external. It is clear that $\tau_{z\theta}$ for all types show discontinuous variation, and the signs of the $\tau_{z\theta}$ are same variations with those of the winding angles. In addition the laminate Seq1 has the lowest values of the stress comparing with the Seq2 and Seq3.

3.1.3 Radial stress

Figure 4 shows the distribution of radial stress σr through the thickness of hybrid solution. The behaviour of radial stress through the thickness indicates the presence of maximal compression of –10 MPa in the internal wall and minimal (equal to zero) in the external wall for all the studied.

In addition, the distribution show nearly linear variation for the three sequences. The curves of radial stress σr for the laminates of the first and second sequence are below than the sequence of the third sequence. The distribution shows nearly linear variation for the three sequences. The curves of radial stress σr for the laminate of Seq1 are below than the laminates of the Seq2 and Seq3.

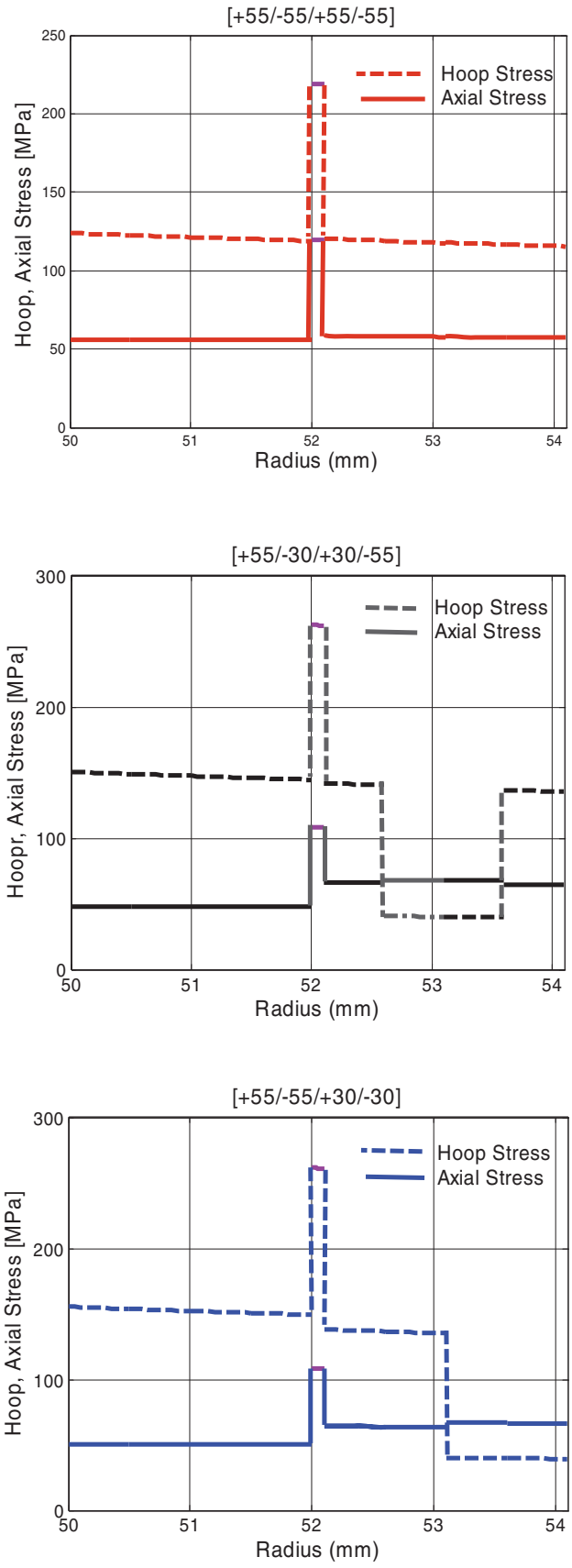

Fig. 2. The distribution of Hoop and axial stress through the thickness.

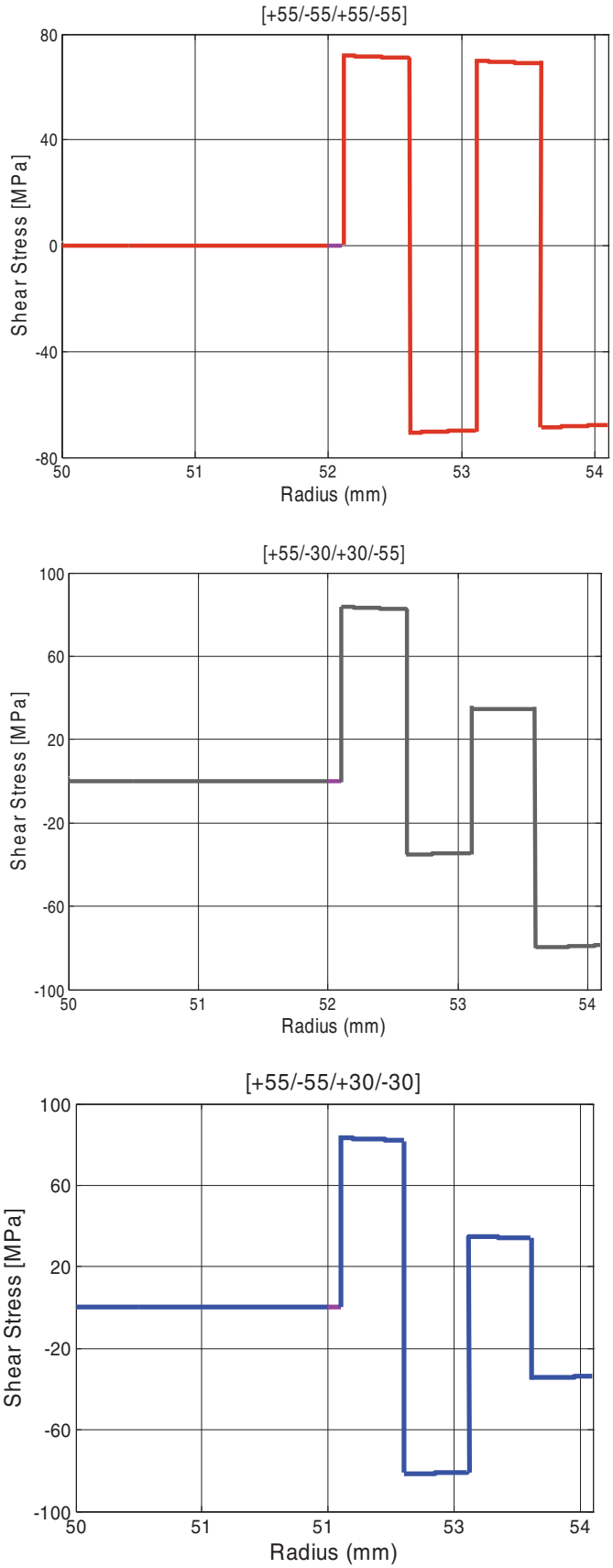

Fig. 3. The distribution of shear stress through the thickness.

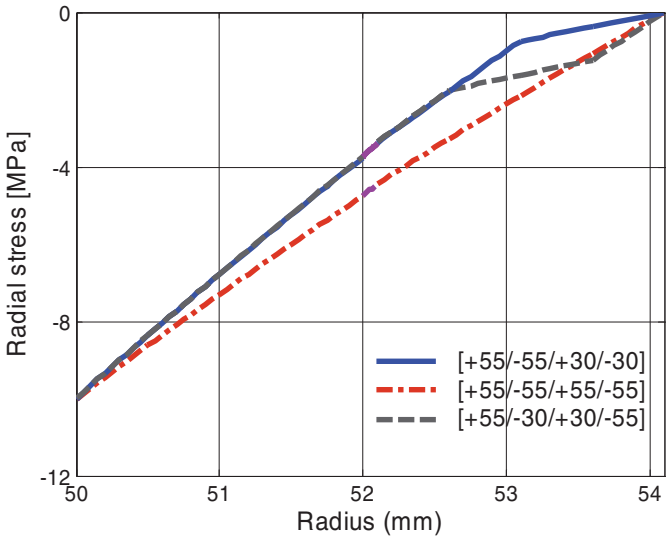

Fig. 4. The distribution of radial stress throught the thickness.

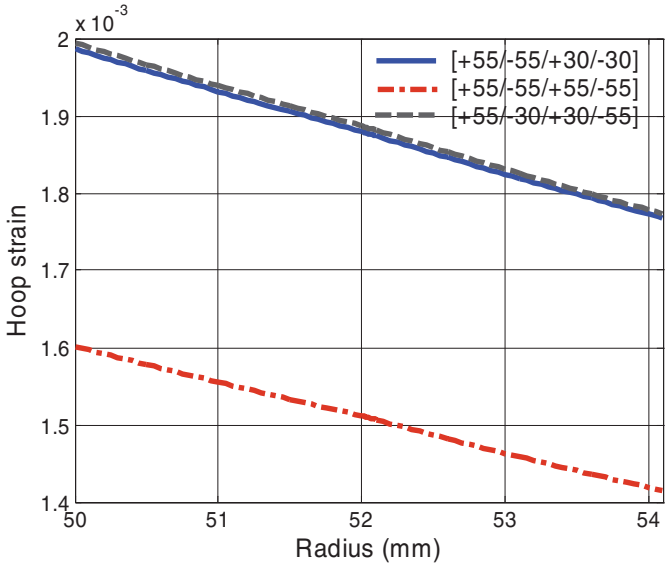

Fig. 5. The distribution of hoop strain through the thickness.

3.2 Strain analysis

➢ Hoop Strain:
Figure 5 shows the hoop strain through the radius of the cylindrical part of the hybrid solution. All hoop stain for the three sequences is characterised by continuous variation from the internal to the external wall. In addition the sequence Seq1 has the *lowest values* of the hoop strain compared with the Seq2 and Seq3.

➢ Radial strain:
Figure 6 shows the radial strain through the radius of the cylindrical part of the hybrid solution. All radial strain for the three sequences is characterised by discontinuous variation at the interfaces from the internal to the external wall. In the part of composite, the sequence Seq2 has the *lowest values* of the hoop strain compared with the Seq1 and Seq3.

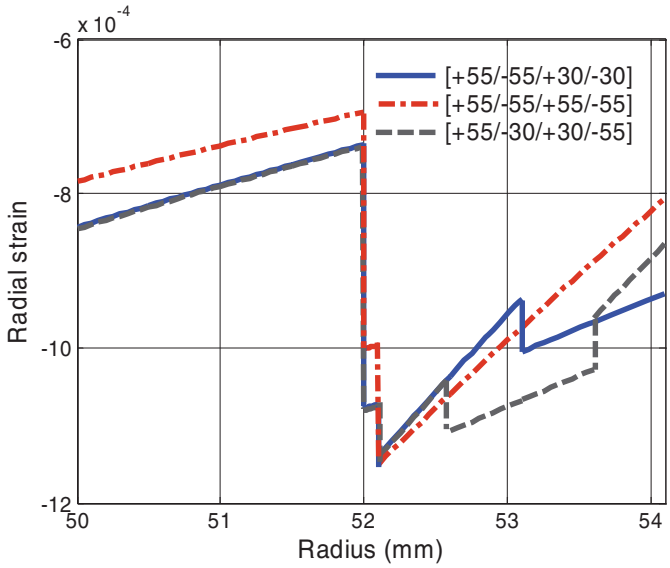

Fig. 6. The distribution of radial strain through the thickness.

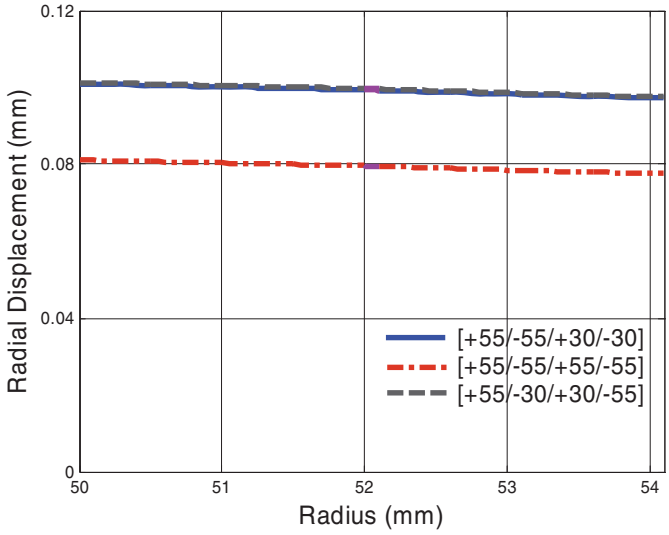

Fig. 7. The distribution of radial displacement through the thickness.

3.2.1 Radial displacement

The variation of radial displacements Ur for the three stacking sequences is shown in Figure 7, where a similar trend for all sequence is observed and the maximum displacements are recorded at the internal wall. Starting from the internal wall, this variation decreases gradually to the minimum value at the external wall. The values of the radial displacement are larger for Seq2 and Seq3 compared to Seq1.

4 Conclusion

The study presents an elastic analytical modelling of a multilayer composite cylindrical tank coated on an aluminium liner and intermetallic for three stacking sequences: [+55/−55/+30/−30], [+55/−55/+55/−55] and

[+55/−30/+30/−55]. This analysis has shown the behaviour of hybrid solution depend strongly on the stacking sequences of the composite. The stacking sequence [+55/−55/+55/−55] presents the best results in term of stresses and displacements compared to other sequences.

The taking into account of the elasto-plastic behavior of the liner will be treated in second part, which is almost completed.

References

1. M. Latroche, *Le stockage de l'hydrogène: Du gaz au solide en passant par le liquide UPR 209* (LCMTR, ISCSA, CNRS, 2-8, rue Henri Dunant, 94320 Thiais, France)
2. M. Junker, L. Bocquet, M. Bendif, D. Karboviac. Ann. Chim. Sci. Mat. **26**, 117 (2001)
3. V.E. Verijenco, S. Adali, Y.P. Tabakov. Composite Structures **54**, 371 (2001)
4. V.V. Vasiliev, A.A. Krinakov, A.F. Razin. Composite Structure **62**, 449 (2003)
5. M. Xia, M. Takayanagi, K. Kemmochi. Composites structures **53**, 483 (2001)
6. D. Chapelle, D. Perreux. International Journal of Hydrogen Energy **31**, 627 (2006)
7. N. Takeichia, H. Senoha, T. Yokotab, H. Tsurutab, K. Hamadab, H.T. Takeshitac, H. Tanakaa, T. Kiyobayashia, T. Takanod, N. Kuriyamaa. International Journal of Hydrogen Energy **28**, 1121 (2003)
8. J.-M. Berthelot, *Composite Materials, Mechanical Behavior and Structural Analysis* (Springer, New York, 1999), p. 676